Quantum Electronics **51** (5) 389–392 (2021)

https://doi.org/10.1070/QEL17543

Possibilities of measuring the exhaled air composition using Raman spectroscopy

D.V. Petrov, I.I. Matrosov, M.A. Kostenko

Abstract. **A Raman spectrometer for gaseous media with a detection limit at a level of 100 ppb is developed. The results of its experimental approval on exhaled air samples from healthy people confirmed the possibility of monitoring the concentrations of a number of hydrocarbon compounds and $^{13}CO_2$. The ways of further development of this analytical method are outlined.**

Keywords: *Raman spectroscopy, gas analysis, exhaled air, diagnostics of diseases.*

1. Introduction

The diagnostics of diseases based on the analysis of the composition of a patient's exhaled air (EA) is a promising direction in modern medicine. This method relies on the fact that EA contains, along with atmospheric components (N_2, O_2, CO_2, and H_2O), trace concentrations of other compounds – products of biochemical processes occurring in a human organism. Many of these compounds (for example, CO, NO, H_2, CH_4, $^{13}CO_2$, C_2H_5OH, C_3H_6O, etc.) have a very high specificity and can be used as biomarkers of diseases [1–3]. This method is attractive primarily due to its noninvasiveness. First, it is safe because it excludes infectious contamination through blood or tools. Second, patients do not experience any physical or emotional discomfort.

To date, the most widespread method for determining the EA composition is gas chromatography–mass spectrometry [4–7]. This approach is characterised by very high sensitivity; however, it requires expendable materials, complex sample preparation, and highly qualified maintenance; in addition, it does not allow one to perform real-time measurements. The methods based on optical spectroscopy are free of these drawbacks. The most popular approach is the diagnostics of EA composition by absorption spectroscopy, with tunable diode IR lasers used as radiation sources [8–11]. This technique is characterised by combination of good selectivity and high sensitivity (to several tenths of ppb). In turn, it has two specific features. First, homonuclear diatomic molecules do not absorb IR radiation. On the one hand, this feature is favourable, because it facilitates identification of impurities against the nitrogen and oxygen background. At the same time, this circumstance does not make it possible to measure, for example, the concentration of hydrogen produced by intestinal bacteria and playing the role of indicator of gastrointestinal tract disorder and problems with malabsorption of hydrocarbons [7, 12–14]. Second, with allowance for the relatively narrow wavelength tuning range, absorption spectroscopy does not make it possible to measure many different gas components using only one emitter–detector pair, which limits significantly its applicability.

Raman spectroscopy is free of the aforementioned drawbacks. The essence of this method is in scattering of excitation laser radiation by molecules of a medium at frequencies determined by their internal structure; the intensity of informative scattering signals is directly proportional to the concentration of scattering molecules. The main advantage of this analytical technique over absorption IR spectroscopy is the possibility of simultaneous monitoring of all molecular components of medium using one laser with a fixed wavelength in the visible range. For a long time the application of this approach in gas analysis was limited, because there was no instrumental base for recording Raman spectra with a high signal-to-noise ratio. However, the situation has changed in the last decade in view of the development of highly sensitive multichannel photodetectors and narrowband holographic filters, as well as the elaboration of technical solutions aimed at increasing the recorded signal intensity [15–19]. As a result, a detection limit at a level of 1 ppm was provided for the method [20–22]. The potential of Raman gas analysis was previously demonstrated by determining the composition of atmospheric air [21, 23] and fuel gases [24–27], using, in particular, the lidar technique [28–30]. In addition, several research teams have described the prospects of this approach for analysing the EA composition [22, 31–33]. Our work is aimed at increasing the sensitivity of this method to a level below 1 ppm and performing its experimental approval on EA samples.

2. Experimental setup

The main problem to solve for a developer of a Raman spectrometer of gas media is to provide a high intensity of informative scattering signals. The most efficient approach in this context is to compress the gas medium under study, because the Raman signal intensity depends almost linearly on pressure [34]. This approach was approved in [20],

D.V. Petrov Institute of Monitoring of Climatic and Ecological Systems, Siberian Branch, Russian Academy of Sciences, prosp. Akademicheskii 10/3, 634055 Tomsk, Russia; Tomsk State University, prosp. Lenina 36, 634050 Tomsk, Russia; e-mail: dpetrov@imces.ru;
I.I. Matrosov, M.A. Kostenko Institute of Monitoring of Climatic and Ecological Systems, Siberian Branch, Russian Academy of Sciences, prosp. Akademicheskii 10/3, 634055 Tomsk, Russia

Received 26 February 2021
Kvantovaya Elektronika **51** (5) 389–392 (2021)
Translated by Yu.P. Sin'kov

where the signal intensity was increased by a factor of about 50. Another approach deserving attention is the increase in intensity as a result of multipass scattering excitation. It was shown in [16, 33] that a signal can be enhanced by a factor of 20 in this way. Taking into account that joint application of these approaches should provide a multiplicative effect, they were laid in the basis of the developed setup, whose scheme is shown in Fig. 1.

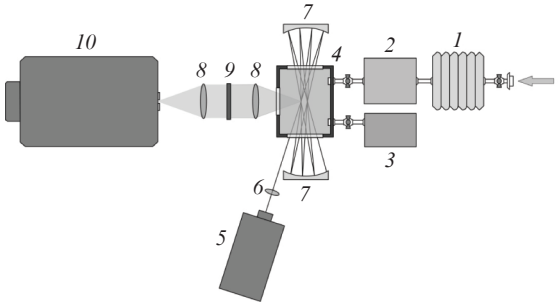

Figure 1. Schematic of the experimental setup: (*1*) air sample container; (*2*) oil-free compressor; (*3*) backing pump; (*4*) gas cell; (*5*) laser; (*6*) lens; (*7*) spherical mirrors; (*8*) lens objectives; (*9*) notch filter; (*10*) spectrometer.

Its principle of operation is as follows. Before each analysis, the entire gas-transport part (including the cell) is evacuated by a backing pump. An EA sample is loaded in a preliminary container, whose volume can be increased to 3 L. This container is connected with an oil-free compressor, which compresses the sample in a 30-cm^3 cell to a pressure of 20 atm. Then a Raman spectrum starts being recorded. The beam of a 5-W cw laser (λ = 532 nm) is directed to the cell, with a multipass optical system (see [33]) mounted at its end faces. As a result of multiple reflections from concentrically located spherical mirrors, two laser-beam intersection regions are formed at the cell centre. Each is a source of scattered light, in which the intensity of excitation beam is proportional to the number of its passes. The scattered radiation is collected by a lens objective with an aperture ratio of 1 : 1.8, spaced from the cell centre by a distance equal to the focal length. Being transmitted through a notch filter (to reduce Rayleigh scattering), the collected radiation is directed (using a similar lens objective) to the input slit of an MKR-2 spectrometer (Sibanalitpribor Ltd., Russia). This instrument equipped with a Hamamatsu S10141 CCD array (512 × 2048 pixels) provides simultaneous spectral measurements in the range of 532–680 nm. Upon excitation of Raman spectra by a 532-nm laser, the aforementioned wavelength band is equivalent to the range of wavenumber shifts from 0 to 4000 cm^{-1}. Working in this range, one can perform simultaneous monitoring of all molecules whose concentrations exceed the threshold value. The estimate of the obtained sensitivity will be given below.

We recorded spectra of two EA samples from two young (30–35 yr) persons without chronic diseases, who did not smoke and had no complaints on health. The EA sample intake time from the last ingestion exceeded 2 h. An examinee took a deep breath directly before sampling and then (without breath delay) a complete exhale, the second half of which was fed to a sample container. In addition, we recorded the spectrum of the air in the room where the experimental setup was mounted, because the examinees breathed in this air. The recording time was 500 s per spectrum.

3. Results and discussion

Figure 2 shows the recorded Raman spectrum of EA. Its main part consists of fundamental nitrogen (2330 cm^{-1}) and oxygen (1555 cm^{-1}) bands, which are saturated because of the limited dynamic range of the detector. The low-wavenumber oxygen wing contains a Fermi dyad of carbon dioxide (1285 cm^{-1}/1388 cm^{-1}). The next in intensity is the water vapour band (3652 cm^{-1}). It is noteworthy that the water vapour was partially condensed due to the sample compression, and the observed band intensity was proportional to the saturated water vapour pressure at room temperature.

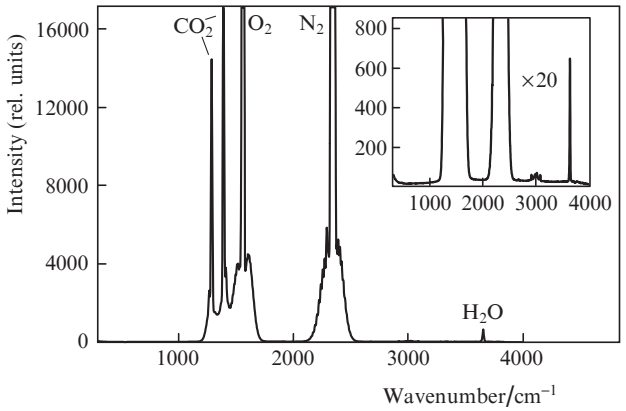

Figure 2. Raman spectrum of exhaled air in the range of 300–4000 cm^{-1}.

The spectra exhibited most significant differences in the range of 2650–3150 cm^{-1} (Fig. 3). The spectrum of atmospheric air contained only an oxygen overtone (3088 cm^{-1}) and a methane peak (2917 cm^{-1}) in this range. The EA spectra exhibited much more peaks, primarily, due to the manifestation of carbon dioxide peaks at 2673, 2990, and 3022 cm^{-1} because of its elevated concentration [35]. Along with this, the methane peak intensity is much higher for both EA samples. Proceeding from its concentration in atmospheric air (2 ± 0.1 ppm), one can conclude that its concentration in EA samples was approximately 9 and 14 ppm. Note that a methane concentration below 10 ppm [36] is considered as normal, whereas an excess above this value is indicative of problems with gastrointestinal tract [12]. In turn, the spectrum of sample 1 as compared with the spectrum of sample 2 is characterised by larger intensity values at wavenumbers of 2887, 2940, 2990, and 3065 cm^{-1}. The wavenumber of 2940 cm^{-1} corresponds acetone, which is rather often present in EA [37, 38]. The peak with a maximum at 2887 cm^{-1} is most likely due to ethanol, which also contributes to the intensity of peak in the vicinity of 2940 cm^{-1}. However, the presence of these two molecules cannot explain the enhanced intensity of the peaks in the range of 2990 and 3065 cm^{-1}. Since this range is characteristic of C–H stretching vibrations, one can state that sample contains some other hydrocarbon compounds; however, their identification calls for a deeper analysis.

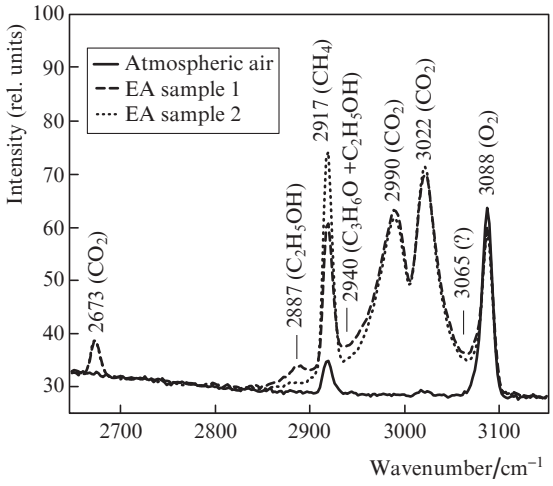

Figure 3. Raman spectra of atmospheric and exhaled air in the range of 2650–3150 cm^{-1}.

Along with the above-considered spectral range, differences between the EA spectra were revealed near the wavenumbers of 1320 and 1370 cm^{-1} against the background of carbon dioxide Fermi dyad (Fig. 4). Since the difference in the intensities exceeded the noise level by more than an order of magnitude, it was due to the difference in the contents of corresponding molecules in the EA samples. The deviation in intensity at a wavenumber of 1370 cm^{-1} indicates a variation in the relative concentration of isotopologue $^{13}CO_2$ [39], which can be within ±3 ‰ for healthy people [40]. In turn, the concentration ratio $^{13}CO_2/^{12}CO_2$ can be used to detect the infection by *Helicobacter pylori* bacteria [8, 11, 41, 42] using a ^{13}C urease test. The difference in the peak intensities at a wavenumber of 1320 cm^{-1} is most likely due to the change in the NO_2 content, which, in turn, is an indicator of pulmonary diseases [43, 44]. Note that we did not perform any exact calculations of variations in the concentrations of the aforementioned components. To this end, it is necessary to correctly take into account the spectra of the dominant components (O_2, CO_2, CH_4, H_2O), which is expedient to do when processing a larger number of EA samples.

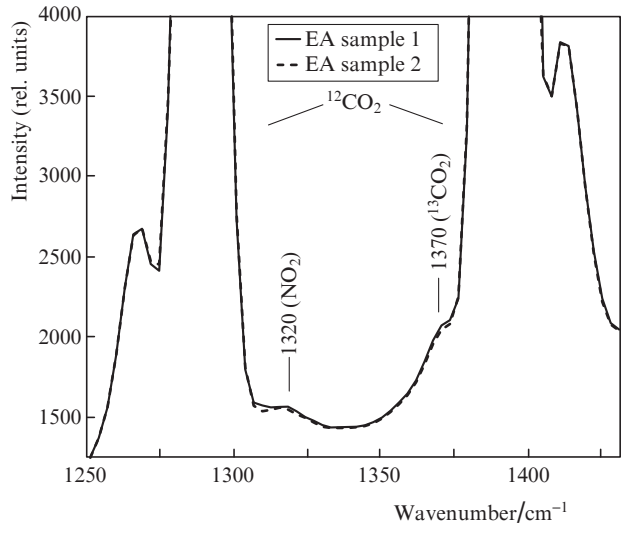

Figure 4. Raman spectra of exhaled air in the range of 1250–1430 cm^{-1}.

Let us estimate the detection limit of the developed experimental setup. In correspondence with the atmospheric air spectrum, the signal-to-noise ratio, defined as the ratio of the peak intensity of the methane band (2917 cm^{-1}) to the rms noise deviation, turned out to be ~20. With allowance for the fact that the methane concentration in atmosphere is about 2 ppm, the detection limit of the system is at the level of 100 ppb. Since each type of molecules has its own scattering cross section [45], the detection limit for them should also differ [25]. However, taking into account that most of hydrocarbon compounds have a scattering cross section close to that for methane or exceeding it, one can state that the detection limit for most of volatile organic compounds in EA is ~100 ppb. According to [2, 3], an instrument with this sensitivity can be used to monitor a number of biomarkers: acetone, carbon oxide, methane, hydrogen, ammonia, isoprene, ethanol, and methanol. It should be noted that this sensitivity can be additionally improved by at least an order of magnitude using a laser of higher power (for example, 10 W), along with a photodetector cooled to –70 °C, and/or increasing the spectrum recording time. As a result, the range of monitored biomarkers can be significantly expanded. At the same time, in the cases where a moderate sensitivity (at a level of 1 ppm) is sufficient, measurements can be performed without sample compression or long exposure times (i.e., one analysis per second can be carried out).

4. Conclusions

We demonstrated the potential of Raman spectroscopy for analysing exhaled air composition. The detection limit of the developed experimental setup turned out to be ~100 ppb for hydrocarbon compounds. Despite the fact that the sensitivity of this method is currently lower than that of absorption spectroscopy, it can be used for complex monitoring of all molecular compounds in analysed air whose concentrations exceed the aforementioned value. This is an advantage over IR sensors; it can be useful when searching for new biomarkers. In turn, to provide a measurement accuracy for molecules of certain types close to that of absorption spectroscopy, the sensitivity must be increased by about two orders of magnitude. It should be noted that the recorded Raman spectra can be applied both for qualitative determination of biomarkers (by comparing the wavenumbers of observed peaks with tabular data or by comparing spectra with reference ones) and for gaining information about the deviations in EA composition without detailed interpretation of spectra using modern processing techniques, such as neural networks and machine learning.

References

1. Popov T.A. *Ann. Allergy, Asthma Immunol.*, **106**, 451 (2011).
2. Buszewski B., Kesy M., Ligor T., Amann A. *Biomed. Chromatogr.*, **21**, 553 (2007).
3. Mazzatenta A., Di C., Pokorski M. *Respir. Physiol. Neurobiol.*, **187**, 128 (2013).
4. Henderson B., Khodabakhsh A., Metsälä M., Ventrillard I., Schmidt F.M., Romanini D., Ritchie G.A.D., Lintel Hekkert S., Briot R., Risby T., Marczin N., Harren F.J.M., Cristescu S.M. *Appl. Phys. B*, **124**, 161 (2018).
5. Kim K.H., Jahan S.A., Kabir E. *Trends Anal. Chem.*, **33**, 1 (2012).
6. Mathew T., Pownraj P., Abdulla S., Pullithadathil B. *Diagnostics*, **5**, 27 (2015).
7. Wang C., Sahay P. *Sensors*, **9**, 8230 (2009).

8. Stepanov E.V. *Quantum Electron*, **32**, 981 (2002) [*Kvantovaya Elektron*., **32**, 981 (2002)].
9. D'yachenko A.I., Stepanov E.V., Shulagin Yu.A. *Opt. Spectrosc.*, **128**, 1048 (2020) [*Opt. Spektrosk*., **128**, 1042 (2020)].
10. Stepanov E.V., Kasoev S.G. *Opt. Spectrosc.*, **126**, 736 (2019) [*Opt. Spektrosk*., **126**, 810 (2019)].
11. Ivashkin V.T., Kasoev S.G., Stepanov E.V. *Opt. Spectrosc.*, **126**, 710 (2019) [*Opt. Spektrosk*., **126,** 788 (2019)].
12. Le Marchand L., Wilkens L.R., Harwood P., Cooney R.V. *Environ. Health Perspect*., **98**, 199 (1992).
13. Rumessen J.J., Nordgaard-Andersen I., Gudmand-Høyer E. *Scand. J. Gastroenterol*., **29**, 826 (1994).
14. Ledochowski M., Widner B., Murr C., Sperner-Unterweger B., Fuchs D. *Scand. J. Gastroenterol*., **36**, 367 (2001).
15. Knebl A., Yan D., Popp J., Frosch T. *Trends Anal. Chem*., **103**, 230 (2018).
16. Schlüter S., Krischke F., Popovska-Leipertz N., Seeger T., Breuer G., Jeleazcov C., Schüttler J., Leipertz A. *J. Raman Spectrosc*., **46**, 708 (2015).
17. Fedorov S.Y., Boyarshinov B.F. *Instr. Exp. Tech*., **60**, 237 (2017).
18. Wang P., Chen W., Wan F., Wang J., Hu J. *Opt. Express*, **27**, 33312 (2019).
19. Petrov D.V., Zaripov A.R., Toropov N.A. *Opt. Lett*., **42**, 4728 (2017).
20. Petrov D.V., Matrosov I.I., Tikhomirov A.A. *J. Appl. Spectrosc*., **82**, 120 (2015).
21. Hanf S., Keiner R., Yan D., Popp J., Frosch T. *Anal. Chem*., **86**, 5278 (2014).
22. Gomez Velez J., Muller A. *Opt. Lett*., **45**, 133 (2020).
23. Petrov D.V., Matrosov I.I., Zaripov A.R. *J. Mol. Spectrosc*., **348**, 137 (2018).
24. Eichmann S.C., Weschta M., Kiefer J., Seeger T., Leipertz A. *Rev. Sci. Instrum*., **81**, 125104 (2010).
25. Petrov D.V., Matrosov I.I., Zaripov A.R., Maznoy A.S. *Appl. Spectrosc*., **74**, 948 (2020).
26. Gao Y., Dai L.-K., Zhu H.-D., Chen Y.-L., Zhou L. *Chinese J. Anal. Chem.*, **47**, 67 (2019).
27. Buldakov M.A., Korolev B.V., Matrosov I.I., Petrov D.V., Tikhomirov A.A. *J. Appl. Spectrosc*., **80**, 124 (2013).
28. Privalov V.E., Shemanin V.G. *Meas. Tech*., **59**, 933 (2016) [*Izmer. Tekh*., No. 9, 22 (2016)].
29. Bobrovnikov S.M., Gorlov E.V., Zharkov V.I. *Atmos. Ocean. Opt*., **26** (4), 320 (2013) [*Opt. Atmos. Okeana*, **26** (1), 70 (2013)].
30. Zhevlakov A.P., Bespalov V.G., Danilov O.B., Zav'yalov A.K., Il'inskii A.A., Kashcheev S.V., Konopel'ko L.A., Mak A.A., Grishkanich A.S., Elizarov V.V. *J. Opt. Technol*., **87**, 11 (2020) [*Opt. Zh*., **87**, 16 (2020)].
31. Chow K.K., Short M., Lam S., McWilliams A., Zeng H. *Med. Phys*., **41**, 092701 (2014).
32. Bögözi T., Popp J., Frosch T. *Bioanalysis*, **7**, 281 (2015).
33. Petrov D.V. *Appl. Opt*., **55**, 9521 (2016).
34. Petrov D.V., Matrosov I.I. *J. Raman Spectrosc.*, **48**, 474 (2017).
35. Tejeda G., Maté B., Montero S. *J. Chem. Phys*., **103**, 568 (1995).
36. Stacewicz T., Bielecki Z., Wojtas J., Magryta P., Mikolajczyk J., Szabra D. *Opto-electronics Rev*., **24**, 82 (2016).
37. Phillips M., Herrera J., Krishnan S., Zain M., Greenberg J., Cataneo R.N. *J. Chromatogr. B Biomed. Sci. Appl*., **729**, 75 (1999).
38. Risby T.H., Solga S.F. *Appl. Phys. B*, **85**, 421 (2006).
39. Howard-Lock H.E., Stoicheff B.P. *J. Mol. Spectrosc*., **37**, 321 (1971).
40. Epstein S., Zeiri L. *Proc. Natl. Acad. Sci. U.S.A*., **85**, 1727 (1988).
41. Crosson E.R., Ricci K.N., Richman B.A., Chilese F.C., Owano T.G., Provencal R.A., Todd M.W., Glasser J., Kachanov A.A., Paldus B.A., Spence T.G., Zare R.N. *Anal. Chem*., **74**, 2003 (2002).
42. Som S., De A., Banik G.D., Maity A., Ghosh C., Pal M., Daschakraborty S.B., Chaudhuri S., Jana S., Pradhan M. *Sci. Rep*., **5**, 1 (2015).
43. Chérot-Kornobis N., Hulo S., Edmé J.L., De Broucker V., Matran R., Sobaszek A. *BMC Res. Notes*, **4**, 202 (2011).
44. Kharitonov S.A., Barnes P.J. *Am. J. Respir. Crit. Care Med*., **163**, 1693 (2001).
45. Schrötter H.W., Klöckner H.W., in *Raman Spectroscopy of Gases and Liquids*. Ed. by A. Weber (Berlin: Springer-Verlag, 1979).